

# Three-dimensional computer analysis of white shark jaw mechanics: how hard can a great white bite?

S. Wroe<sup>1</sup>, D. R. Huber<sup>2</sup>, M. Lowry<sup>3</sup>, C. McHenry<sup>1,4,5</sup>, K. Moreno<sup>1</sup>, P. Clausen<sup>4</sup>, T. L. Ferrara<sup>1</sup>, E. Cunningham<sup>6</sup>, M. N. Dean<sup>7</sup> & A. P. Summers<sup>7</sup>

<sup>1</sup> School of Biological, Earth and Environmental Sciences, University of New South Wales, Sydney, Australia

<sup>2</sup> Department of Biology, University of Tampa, Tampa, FL, USA

<sup>3</sup> NSW Department of Primary Industries (Research Division), Cronulla, NSW, Australia

<sup>4</sup> School of Engineering, University of Newcastle, Newcastle, NSW, Australia

<sup>5</sup> School of Environmental and Life Sciences, University of Newcastle, Newcastle, NSW, Australia

<sup>6</sup> Newcastle Mater Misericordiae Hospital, Newcastle, NSW, Australia

<sup>7</sup> Ecology and Evolutionary Biology, University of California, Irvine, CA, USA

## Keywords

finite element analysis; bite force;  
*Carcharodon carcharias*; *megalodon*.

## Correspondence

Stephen Wroe, School of Biological, Earth and Environmental Sciences, University of New South Wales, Sydney 2052, Australia.  
Email: s.wroe@unsw.edu.au

Editor: Andrew Kitchener

Received 24 April 2008; revised 20 June 2008; accepted 30 June 2008

doi:10.1111/j.1469-7998.2008.00494.x

## Abstract

The notorious jaws of the white shark *Carcharodon carcharias* are widely feared, yet poorly understood. Neither its bite force, nor how such force might be delivered using relatively elastic cartilaginous jaws, have been quantified or described. We have digitally reconstructed the jaws of a white shark to estimate maximum bite force and examine relationships among their three-dimensional geometry, material properties and function. We predict that bite force in large white sharks may exceed *c.* 1.8 tonnes, the highest known for any living species, and suggest that forces may have been an order of magnitude greater still in the gigantic fossil species *Carcharodon megalodon*. However, jaw adductor-generated force in *Carcharodon* appears unremarkable when the predator's body mass is considered. Although the shark's cartilaginous jaws undergo considerably greater deformation than would jaws constructed of bone, effective bite force is not greatly diminished.

## Introduction

The threatened white shark *Carcharodon carcharias*, is the world's largest extant predatory fish. Its gigantic, whale-eating relative, *Carcharodon megalodon*, was arguably the most formidable carnivore ever to have existed (Gottfried, Compagno & Bowman, 1996; Purdy, 1996). Unsurprisingly, the biology of *Carcharodon* has received much attention (e.g. Klimley & Ainley, 1998; Boustany *et al.*, 2002), but bite force and the mechanical behaviour of its feeding apparatus, key factors in understanding feeding ecology and form–function relationships in sharks and other vertebrates (Huber & Motta, 2004; Huber *et al.*, 2005; Wroe, McHenry & Thomason, 2005; Christiansen & Wroe, 2007) have remained largely unknown. This lack of information has led to considerable speculation regarding white shark feeding performance, which has in turn influenced public perceptions.

Further uncertainty regarding *Carcharodon*, and chondrichthyan fish in general, concerns the influence of relatively compliant cartilage (compared with bone) as the structural basis for their feeding mechanisms (Summers, 2000). Chondrichthyan cartilage is several orders of magni-

tude less stiff than vertebrate bone (Summers & Long Jr 2006). Thus, questions are warranted regarding both the effectiveness of cartilage as a force-transmitting material in musculoskeletal lever systems and its ability to withstand loading. Answers will be fundamental to understanding the radiation of chondrichthyan fishes beginning over 450 mya (Turner, 2004) and to shed light on the role of chondrichthyan fish as apex predators in virtually all marine ecosystems.

We have investigated the bite force and mechanical behaviour of the jaw cartilages of the white shark using a finite element (FE) approach, building and analyzing computer simulations based on serial computed tomography (CT) with inputs determined on the basis of *in vivo* data (Fig. 1). FE has emerged as a powerful tool for the examination of form and function for both living and extinct species (Thomason, 1995; Rayfield *et al.*, 2001; McHenry *et al.*, 2007; Wroe *et al.*, 2007a; Moreno *et al.*, 2008), and is an asset for studying experimentally intractable organisms such as *Carcharodon*. FE-derived results for bite force were also compared with those generated using a more traditional, empirically validated method after Huber *et al.* (2005), using a three-dimensional (3-D) static equilibrium model to estimate maximum theoretical bite force.

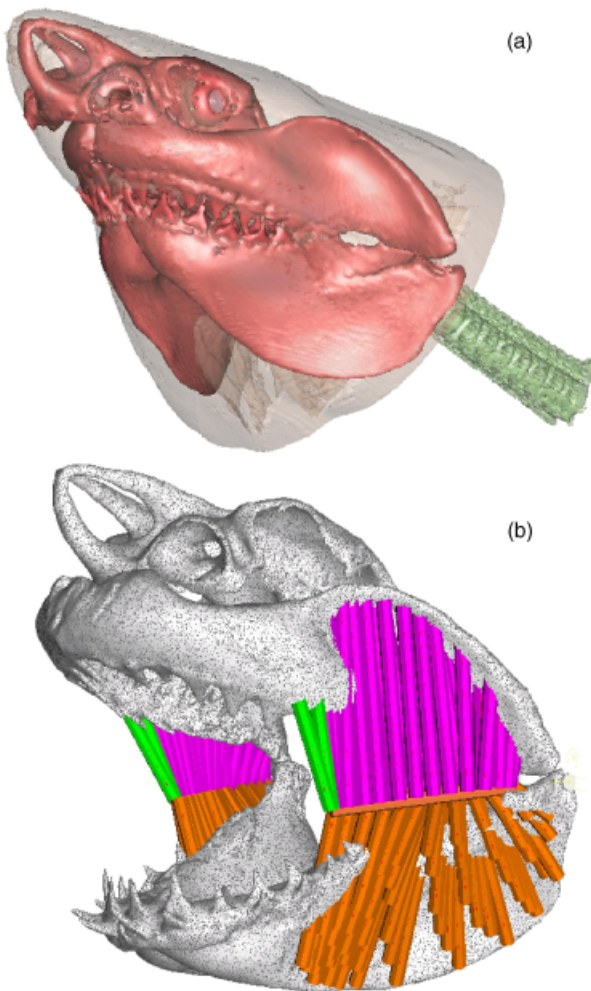


**Figure 1** (a) Three-dimensional object assembled from computed tomography scan data totaling 237 slices of *Carcharodon carcharias*. (b) 1.94 million tetrahedral three-dimensional ‘brick’ finite element model of the same specimen showing jaw adducting musculature: preorbitalis (green), quadratomandibularis dorsal (pink) and ventral (orange) divisions. Muscles simulated using 256 pretensioned trusses connected to central beams.

## Materials and methods

### Overview

Analyses are based on 3-D FE models of the chondrocranium and jaws of a 2.5 m, 240 kg specimen of *C. carcharias* (NSWDPI-WS2006/4), assembled from CT scan data (Fig. 1). Model construction largely followed recently developed protocols (McHenry *et al.*, 2007; Wroe, 2007; Wroe *et al.*, 2007a).

Four FE models of the feeding mechanism of *C. carcharias* were constructed. A heterogeneous cartilage model was assigned multiple material properties based on CT scan density data (see ‘Material properties’). In order to assess the degree to which the use of relatively compliant cartilage

might influence maximal bite forces, a second homogeneous model was assembled. This simulation assumed a single stiffness for cortical bone, with a Young’s Modulus of 27.08 GPa and a Poisson’s ratio of 0.4 (McHenry *et al.*, 2007; Wroe *et al.*, 2007b). In these two models, each muscle was modeled with multiple trusses in order to distribute forces more realistically (see the loading cases below). Gape angle in both instances was set at 35° based on observation of still images of prey capture (Martin *et al.*, 2005).

A second heterogeneous model was assembled with gape at 0° to facilitate comparison of bite force results with those obtained applying the methodology of Huber *et al.* (2005). Muscles were modeled as in the above two instances. In a third heterogeneous simulation (gape at 0°), each muscle was modeled as a single truss to still more closely approximate the methodology of Huber *et al.* and examine the effect of using multiple as opposed to single muscle vectors.

Each FE model comprised 1.94 million tetrahedral 3-D ‘brick’ elements assembled using Strand7 (Vers. 2.3) FE software. Our methods allowed inclusion of multiple material properties and 3-D simulation of force production by the jaw adducting musculature (Wroe, 2007; Wroe *et al.*, 2007a,b), with the jaw joint modeled as in Wroe (2007).

The relationship between muscle force (a function of area) and body mass (a function of volume) is negatively allometric and described by a two-thirds power rule. For most taxa, including sharks, this holds true for bite force (Huber *et al.*, 2005). Our estimates for bite force in larger specimens of *Carcharodon* assume that bite force increases at 0.67 the power of body mass relative to the modeled specimen.

### Material properties

For heterogeneous models, individual elements were designated as one of eight material property types, based on X-ray attenuation (measured in Hounsfield Units, HU) of the corresponding voxels within the CT scan data (McHenry *et al.*, 2007; Wroe, 2007). Elements were assumed to be isotropic. For each element, the HU was converted to density ( $\rho$ ) (Rho, Hobatho & Ashman, 1995; Schneider, Pedroni & Lomax, 1996; McHenry *et al.*, 2007); see Table 1 for absolute values. The relationship between  $\rho$  and Young’s modulus ( $E$ ) is different for cartilage than for bone, and values for  $E$  in chondrichthyan prismatic calcified and extra-cellular cartilage were used to derive an equation relating  $\rho$  to  $E$  ( $E = 0.0014\rho^{2.054}$ ). For a given value of  $\rho$ ,  $E$  in cartilage is substantially less than values for bone (Table 1).

The material properties of the calcified and uncalcified portions of the tessellated elasmobranch skeleton (Dean & Summers, 2006) were determined over very fine linear scales using a Nanoindenter XP (Berkovich, Nanoinstruments Innovation Center, MTS Systems, TN, USA) with the pyramidal tip displaced 500–1000 µm into cross-sections of round stingray *Urotrygon halleri* tissue. Values for  $E$  of uncalcified cartilage were further estimated via stress-relaxation tests of cylindrical cartilage samples from horn *Heterodontus francisci*, lemon *Negaprion brevirostris* and blacktip

**Table 1** Values used to assign material properties to elements in a heterogeneous model

Material property type	Mean (HU)	Density ( $\text{kg m}^{-3}$ )	Young's modulus (MPa) – chondrichthyan cartilage	Young's modulus (MPa) – mammalian bone
1	-825	75.06	9.96	308.92
2	-427	115.43	24.09	546.56
3	-29	155.79	44.60	813.44
4	369	694.78	961.62	5906.40
5	768	1233.78	3127.68	12 647.69
6	1166	1432.84	4252.50	15 422.30
7	1564	1631.91	5554.98	18 325.82
8	1962	1830.97	7036.37	21 347.37

The HU values are used to assign density (McHenry *et al.*, 2007; Wroe *et al.*, 2007a,b). Density values are converted to values for Young's modulus using data for shark cartilage – values of modulus for mammalian bone (McHenry *et al.*, 2007) are shown for comparison. HU, Hounsfield units.

*Carcharhinus limbatus* sharks. Samples were axially compressed to 25% strain for 2 mins on an MTS 858 Material Testing System (MTS Systems Corporation, Eden Prairie, MN, USA) with a 500 N load cell.  $E$  was estimated from the upper 75% of the elastic region of the stress-strain curve. The mean  $E$  and Poisson's ratio for calcified cartilage were 4.05 GPa and 0.30, respectively, whereas those for uncalcified cartilage were 55.1 MPa and 0.30, respectively.

## Muscle forces

*In vivo* data on muscle geometry were collected from NSW DPI-WS2006/4 and a maximal bilateral muscle force of 4532 N was calculated in accordance with the methods of Huber *et al.* (2005). The theoretical maximum tetanic tension ( $P_O$ ) of each muscle was estimated by multiplying its anatomical cross-sectional area ( $A_{CS}$ ) by the specific tension ( $T_{SP}$ ) of elasmobranch white muscle [289 kN m $^{-2}$  (Lou, Curtin & Woledge, 2002)]:

$$P_O = A_{CS} \times T_{SP}$$

$A_{CS}$  was measured using Sigma Scan Pro 4.01 (Systat Software Inc., Point Richmond, CA, USA) from digital images of cross-sections taken through the center of mass, perpendicular to the principal muscle fiber direction. Bilateral forces were 1642, 2772 and 118 N for the dorsal quadratomandibularis, ventral quadratomandibularis and preorbitalis, respectively.

## Loading cases

Analyses were linear static. Muscles were modeled as pretensioned trusses that thereby provided a means of applying forces as well as determining force vectors. Truss numbers were proportional to muscle origin areas (McHenry *et al.*, 2007). Respective pretensions applied to these trusses and truss numbers for each muscle were 13.03 N, 126 (dorsal

quadratomandibularis); 22.00 N, 128 (ventral quadratomandibularis) and 29.50 N, four (preorbitalis). The mid-lateral raphe of the quadratomandibularis, to which each of these muscles attach, was simulated using a divided beam (Fig. 1). Fixed nodes at the anterior-most and posterior-most extremes of these two beams represented the only constraints aside from bite points.

Both the heterogeneous models comprising calcified and uncalcified cartilage and the hypothetical homogeneous model (constructed of cortical bone) were subjected to loads simulating maximal bilateral muscle activation at a 35° gape angle with resulting bites at four nodes (one on each side of both the upper and the lower jaws). These bite points were at either 75 or 50% of the total jaw length anterior to the jaw joint, functionally representing anterior and posterior biting, respectively. Together with reaction forces, the mean Von Mises 'brick' element stress, strain and displacement were calculated from these simulations. Bite force was also taken from the two 0° gape angle simulations for comparison with the static equilibrium model.

## Results

At a gape angle of 35°, our heterogeneous FE model of the 2.5 m, 240 kg white shark generated an anterior bite force of 1602 N and a posterior bite force of 3131 N. Modeling at a gape angle of 0° during an anterior bite in the heterogeneous model with multiple trusses distributing loads for each muscle yielded a bite force of 1393 N, and that in which muscles were modeled using single trusses yielded a figure of 934 N. Applying the approach of Huber *et al.* (2005) yielded an anterior bite force of 1018 N.

Assuming isometry, scaling the 35° gape angle data for a 6.4 m, 3324 kg white shark yields maximum anterior and posterior bite forces of 9320 and 18 216 N, respectively (Table 2). Applying this methodology to mass estimates of *C. megalodon* places this gigantic carnivore's bite force at

**Table 2** Bite force for great white and megatooth sharks

	Body mass (kg)	Scaling factor	Anterior bite force (N)	Posterior bite force (N)
<i>Carcharodon carcharias</i>	240	–	1602	3131
<i>C. carcharias</i> <sup>a</sup>	423	1.46	2341	4577
<i>C. carcharias</i> <sup>b</sup>	3324	5.82	9320	18 216
<i>Carcharodon megalodon</i> <sup>c</sup>	47 690	34.81	55 522	108 514
<i>C. megalodon</i> <sup>d</sup>	103 197	58.13	93 127	182 201

<sup>a</sup>Minimum body mass at sexual maturity based on total length data.

<sup>b</sup>Largest verified body mass of *C. carcharias* (Tricas & McCosker, 1984).

<sup>c</sup>Conservative maximum body mass (Gottfried, Compagno & Bowman, 1996).

<sup>d</sup>Maximum body mass (Gottfried, Compagno & Bowman, 1996).

Bite force estimates for a, b, c and d based on two-thirds power rule relationship between muscle force and body mass (Liem *et al.*, 2001).

between 55 522 and 93 127 N in an anterior bite and between 108 514 and 182 201 N in a posterior bite (Table 2).

While these figures are considerable in absolute terms, where comparable, they are not high relative to mammals or reptiles of similar size. For example, applying a similar FE methodology, computation of the maximal anterior bite force in a 267 kg African lion yields a figure of *c.* 3300 N (McHenry *et al.*, 2007), that is, more than twice that of a 240 kg white shark.

The results for stress, strain and displacement are shown in visual plots (Figs 2 and 3). The mean 'brick' element values for stress (Fig. 2) are lower in our more realistic, cartilaginous simulation of the white shark's jaws (2.12 MPa) than for hypothetical jaws assigned properties for cortical bone (3.04 MPa). The reverse is true with respect to mean 'brick' element strain (Fig. 2), with the cartilaginous model recording 1.29E-02 mm mm<sup>-1</sup> as opposed to 1.57E-04 mm mm<sup>-1</sup> in the homogeneous simulation. The greatest displacement was around the jaw joints. At *c.* 47.5 mm, this was over 70 times greater in the cartilaginous model than was generated in the cortical bone model (Fig. 3). The least displacement was at the anterior tips of the jaws at <2.9 mm. Effective bite force was 4.4% higher in the hypothetical 'bone' jaws in an anterior bite (1672 vs. 1602 N).

## Discussion

Feeding behaviors and kinematics are complex in sharks (Motta *et al.*, 2002). A full bite sequence may involve five

distinct components: cranial elevation, lower jaw depression and upper jaw protrusion, followed by lower jaw elevation and head depression. Moreover, ram feeding behaviors by *C. carcharias* may vary considerably depending on factors including the type, size and depth of prey (Tricas, 1985). Modeling presented here is limited to the prediction of mechanical behavior in relation to lower jaw elevation. Some observed behaviors, such as lateral shaking (Martin *et al.*, 2005), might incorporate significant postcranially generated forces. These could amplify readings recorded at the bite points in our model as has been found in some mammalian carnivores (McHenry *et al.*, 2007). Thus, depending on how bite force is defined, it is likely that the total delivered forces experienced by prey are higher than those estimated here.

Gape angle clearly impacts bite force, which was lower when modeled at 0° in the FE models. Although at 35° mechanical advantage is probably approaching its optimum, modeling at a wider range of gape angles will be required to establish absolute maximal jaw adductor-driven bite force (Bourke *et al.*, 2008).

Nonetheless, when modeling at a gape of 0°, our FE-based result for the model with multiple trusses for each muscle was considerably higher than that obtained using the static equilibrium approach of Huber *et al.* (2005) at the same angle (1018 N). Comparable differences with FE-based results, wherein muscles were approximated using multiple pretensioned trusses, have yielded bite forces approaching or exceeding 30% higher than those obtained using simpler 2-D approaches (McHenry *et al.*, 2007; Wroe,

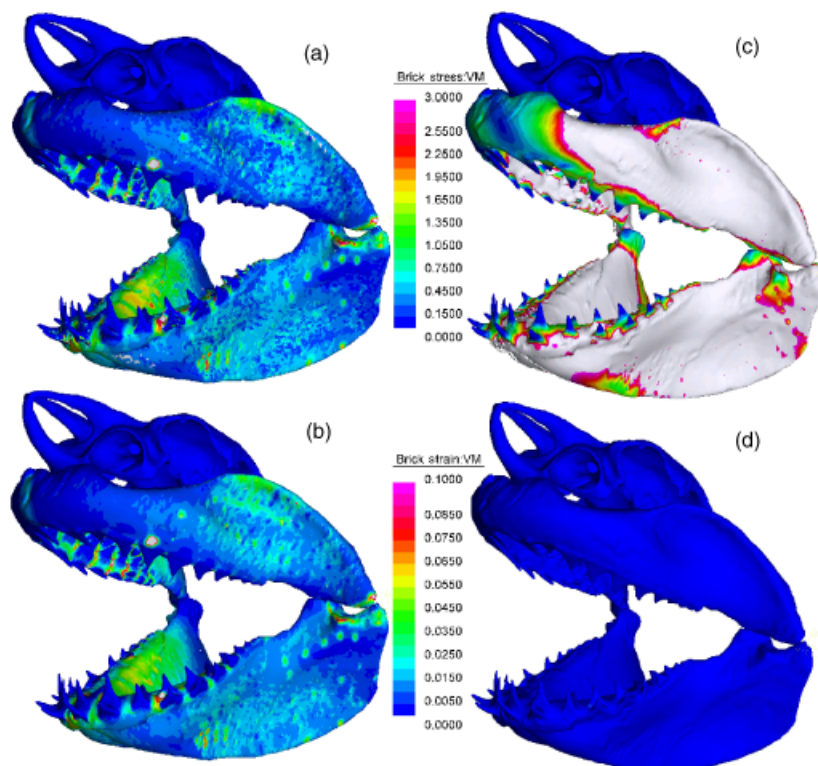


**Figure 2** Von Mises stress (a, c) and strain (b, d) distributions for maximal bilateral bites in simulations using heterogeneous, eight-property cartilaginous jaws (a, b) and homogeneous jaws assigned a single property for cortical bone (c, d). Note that stress is much lower in the cartilaginous model, but strain is much higher in heterogeneous than in homogeneous simulations.

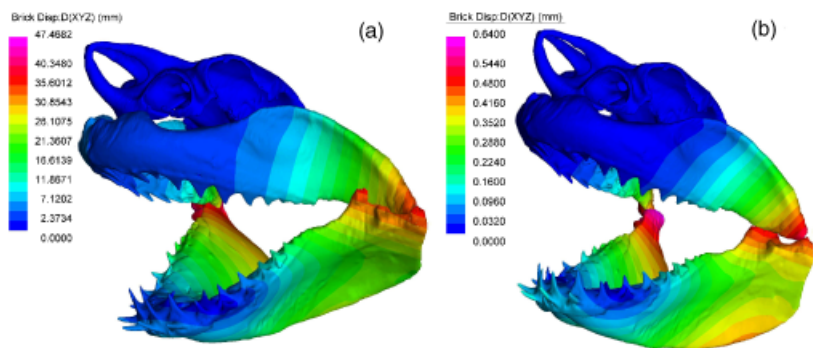


**Figure 3** (a) Displacement for maximal bilateral bites in simulations using heterogeneous, eight-property cartilaginous jaws and homogeneous jaws assigned a single property for cortical bone. (b) Absolute displacement amplified by a factor of  $1.5 \times$  in both models. Despite much greater deformation, the bite force is only slightly lower in the more realistic simulation incorporating material properties for cartilage than in the hypothetical and far stiffer homogeneous simulation (i.e. 1602 vs. 1672 N).

2007). Huber *et al.* (2005), as well as the static equilibrium analysis presented here, simplify lines of action for each of the primary adductors to single vectors, whereas our FE models more realistically spread loads across origin and insertion points using multiple vectors. Because the second, less realistic  $0^\circ$  gape FE simulation (muscles modeled as single vectors) gave a bite force much closer to that using the approach of Huber *et al.* (2005), we consider it probable that muscle architecture in the more realistic simulation imparts greater mechanical advantage.

Bite force adjusted for body mass correlates with relative prey size in extant mammalian carnivores (Wroe *et al.*, 2005; Christiansen & Wroe, 2007). However, this relationship does not necessarily hold for extinct predators with morphologies that differ markedly from those of living taxa (Wroe *et al.*, 2005). The sabre-toothed cat *Smilodon fatalis*, is one such example (McHenry *et al.*, 2007), and killing tactics used by white sharks have been broadly likened to those hypothesized for *S. fatalis* (Diamond, 1986). It has been suggested that both taxa apply behaviors wherein lethal physical trauma is rapidly induced by a single bite into soft tissue, minimizing the risk of injury to the predator from struggling prey (Diamond, 1986; McHenry *et al.*, 2007). In the white shark, this entails a high-speed ambush of typically pinniped prey, followed by a period of prey exsanguination during which the white shark waits for its meal on the periphery (Martin *et al.*, 2005).

Interestingly, results of FE modeling suggest that jaw adductor-generated bite force in *S. fatalis* is also relatively weak (*c.* 1100 N in an anterior bite for a 229 kg animal), but indicate that postcranially generated forces may have played an important role in the kill (McHenry *et al.*, 2007). Further analogy might be drawn in that the killing teeth of both sabretooth and shark are sharp compared with the robust, conical killing teeth of many other large predators, including pantherine cats, most extant crocodylians and many living and extinct marine predators.

A number of other taxa that are known or thought to take relatively large prey that are also characterized by sharp, relatively gracile teeth, also appear to generate relatively weak bite forces, for example, allosauroid dinosaurs (Rayfield *et al.*, 2001) and some monitor lizards (Moreno *et al.*, 2008). Thus, while bite force may be a useful predictor of relative prey size for conical-toothed carnivores

across a wide range of taxa, this will not directly apply to species possessing gracile, laterally compressed teeth. However, it remains to be seen whether higher bite forces might correlate with relatively larger prey within subsets of sharp-toothed taxa. Additionally, the interaction between the high absolute bite forces and sharp dentitions of these predators likely exceeds the mechanical constraints imposed by prey connective tissues, thus relaxing selective pressure for high mass-specific bite forces at large body sizes (Huber *et al.*, 2008).

Our maximal bite force prediction of 18 216 N for the largest white shark is the highest thus far calculated for any living species, and among the highest if comparison is extended to extinct taxa (discussed below). At 108 514–182 201 N, our estimated maximum bite force in *C. megalodon* is extraordinary. These huge forces must be considered in the context of the great size of this fossil predator (maxima of 48 000–103 000 kg) and paleontological evidence suggesting that megatooth was an active predator of large whales (Purdy, 1996). A predominance of tooth marks on tail vertebrae and flipper bones (Purdy, 1996) suggests that this giant shark first immobilized its leviathan prey before feeding.

With respect to previous estimates of bite force in gigantic taxa, a bite force of 5300 N has been proposed for the Devonian placoderm fish *Dunkleosteus terrelli* (Anderson & Westneat, 2007), and using a reverse engineering approach it has been calculated that a bite force of 13 400 N was required for a large maxillary tooth of *Tyrannosaurus rex* to cause measurable damage to the pelvis of a *Triceratops* (Erickson *et al.*, 1996). The assumption that all potentially biting teeth were similarly loaded yields a figure of 156 120 N (Rayfield, 2004), a figure of a magnitude comparable to the estimate of 183 000–235 000 N for *T. rex* obtained by Meers (2003) based on the scaling relationship of bite force to body mass in extant reptilian and mammalian carnivores. However, although the skull of *T. rex* was clearly adapted to offer considerable resistance (Snively, Henderson & Phillips, 2006), it is unlikely that all teeth would have contacted a prey item simultaneously and if force is scaled for tooth size, then bite force for *T. rex* in this instance was 31 000 N (Rayfield, 2004). Furthermore, it is impossible to determine whether this force was generated solely by jaw adducting musculature or amplified by cervical or other postcranial

muscles. Regardless, in terms of bite force, if the assumptions of our scaling analysis are valid, *C. megalodon* is clearly one of the most powerful predators in vertebrate history.

Our finding that mean brick stress was considerably lower while strain and displacement were much higher in the cartilaginous simulation than in the hypothetical ‘bone’ simulation of the white shark’s jaws was not unexpected. However, the relatively small difference in recorded reaction forces between the two simulations suggests that, theoretically, the use of cartilage is no great impediment to the generation of high bite forces. On the other hand, whether the shark’s cartilaginous jaws could withstand the strains recorded in the present analysis, particularly at the jaw joint, remains to be determined.

While we believe that the approach applied here represents an important step towards a fuller understanding of shark biomechanics, as with all modeling methods, the veracity of results is dependent on the validity of various assumptions. The most obvious of these include those that moduli of elasticity and muscle forces in *Carcharodon* approximate those of other cartilaginous fish used as proxies here. Moreover, our modeling assumes isotropy, whereas it is likely that some anisotropy characterizes the jaws of all large sharks (although it is worth reiterating here that at least with respect to bite force, major differences between cartilaginous and hypothetical ‘bone’ simulations have relatively little impact on results). Regarding larger *Carcharodon*, the further assumption of a two-third power relationship between bite force and body mass is reasonable based on first principles of geometric scaling and supported in part by previous work (Huber *et al.*, 2005). However, the fact remains that the largest specimens to which we have extended this assumption lie well beyond the verifiable data range, particularly in the case of *C. megalodon*.

With respect to such large, rare and potentially dangerous animals, full validation is unlikely to be ever achieved and is impossible in the case of extinct taxa. However, it is hoped that work in progress will offer further validation in smaller shark species and this will improve confidence in the results of such analyses.

## Acknowledgements

This work was funded by Australian Research Council, University of New South Wales Internal Strategic Initiatives, and Australia and Pacific Science Foundation Grants to S.W.

## References

- Anderson, P.S.L. & Westneat, M.W. (2007). Feeding mechanics and bite force modelling of the skull of *Dunkleosteus terrelli*, an ancient apex predator. *Biol. Lett.* **3**, 76–79.
- Bourke, J., Wroe, S., Moreno, K., McHenry, C. & Clausen, P. (2008). Effects of gape and tooth position on bite force in the Dingo (*Canis lupus dingo*) using a 3-D finite element approach. *PLoS ONE* **3**, 1–5.
- Boustany, A.M., Davis, S.F., Pyle, P., Anderson, S.D., Le Boeuf, B.J. & Block, B.A. (2002). Satellite tagging: expanded niche for white sharks. *Nature* **415**, 35–36.
- Christiansen, P. & Wroe, S. (2007). Bite forces and evolutionary adaptations to feeding ecology in carnivores. *Ecology* **88**, 347–358.
- Dean, M.N. & Summers, A.P. (2006). Cartilage in the skeleton of cartilaginous fishes. *Zoology* **109**, 164–168.
- Diamond, J. (1986). How great white sharks, sabre-toothed cats and soldiers kill. *Nature* **322**, 773–774.
- Erickson, G.M., Van Kirk, S.D., Jinntung, S., Levenston, M.E., Caler, W.E. & Carter, D.R. (1996). Bite-force estimation for *Tyrannosaurus rex* from tooth-marked bones. *Nature* **382**, 706–708.
- Gottfried, M.D., Compagno, L.J.V. & Bowman, C. (1996). Size and skeletal anatomy of the giant “megatooth” shark *Carcharodon megalodon*. In *Great white sharks: the biology of Carcharodon carcharias*: Vol. 55, 55–66. Klimley, A.P. & Ainley, D.G. (Eds). San Diego, CA, USA: Academic Press.
- Huber, D.R., Claes, J.M., Mallefet, J. & Herrel, A. (2008). Is extreme bite performance associated with extreme morphologies in sharks? *Physiol. Biochem. Zool.* (in press).
- Huber, D.R., Eason, T.G., Hueter, R.E. & Motta, P.J. (2005). Analysis of the bite force and mechanical design of the feeding mechanism of the durophagous horn shark *Heterodontus francisci*. *J. Exp. Biol.* **208**, 3553–3571.
- Huber, D.R. & Motta, P.J. (2004). Comparative analysis of methods for determining bite force in the spiny dogfish *Squalus acanthias*. *J. Exp. Zool.* **301A**, 26–37.
- Klimley, A.P. & Ainley, D.G. (1998). *Great white sharks: the biology of Carcharodon carcharias*. San Diego, CA: Academic Press.
- Liem, K.F., Bemis, W.E., Walker, W.F. & Grande, L. (2001). *Functional morphology of the vertebrates*, 3rd edn. Belmont: Brooks/Cole.
- Lou, F., Curtin, N.A. & Woledge, R.C. (2002). Isometric and isovelocity contractile performance of red muscle fibers from the dogfish *Scyliorhinus canicula*. *J. Exp. Biol.* **205**, 1585–1595.
- Martin, R.A., Hammerschlag, N., Collier, R.S. & Fallows, C. (2005). Predatory behaviour of white sharks (*Carcharodon carcharias*) at Seal Island, South Africa. *J. Mar. Biol. Assoc. (UK)* **85**, 1121–1135.
- McHenry, C.R., Wroe, S., Clausen, P.D., Moreno, K. & Cunningham, E. (2007). Supermodeled sabercat, predatory behavior in *Smilodon fatalis* revealed by high-resolution 3D computer simulation. *Proc. Natl. Acad. Sci.* **104**, 16010–16015.
- Meers, M.B. (2003). Maximum bite force and prey size of *Tyrannosaurus rex* and their relationships to the inference of feeding behaviour. *Hist. Biol.* **16**, 1–12.
- Moreno, K., Wroe, S., Clausen, P.D., McHenry, C.R., D’Amore, D. & Rayfield, E. (2008). Cranial performance in the Komodo dragon (*Varanus komodoensis*) as revealed by

- high-resolution 3-D finite element analysis. *J. Anat.* **212**, 736–746.
- Motta, P.J., Hueter, R.E., Tricas, T.C. & Summers, A.P. (2002). Kinematic analysis of suction feeding in the Nurse Shark, *Ginglymostoma cirratum* (Orectolobiformes, Ginglymostomatidae). *Copeia* **1**, 24–38.
- Purdy, R.W. (1996). Paleoecology of fossil white sharks. In *Great white sharks: the biology of Carcharodon carcharias*: Vol. 67, 67–78. Klimley, A.P. & Ainley, D.G. (Eds). San Diego: Academic Press.
- Rayfield, E.J. (2004). Cranial mechanics and feeding in *Tyrannosaurus rex*. *Proc. Roy. Soc. Lond. Ser. B* **271**, 1451–1459.
- Rayfield, E.J., Norman, D.B., Horner, C.C., Horner, J.R., Smith, P.M., Thomason, J.J. & Upchurch, P. (2001). Cranial design and function in a large theropod dinosaur. *Nature* **409**, 1033–1037.
- Rho, J.Y., Hobatho, M.C. & Ashman, R.B. (1995). Relations of mechanical properties to density and CT numbers in human bone. *Med. Eng. Physiol.* **17**, 347–355.
- Schneider, U., Pedroni, E. & Lomax, A. (1996). The calibration of CT Houndsfield units for radiotherapy treatment planning. *Phys. Med. Biol.* **41**, 111–124.
- Snively, E., Henderson, D.M. & Phillips, D.S. (2006). Fused and vaulted nasals of tyrannosaurid dinosaurs: implications for cranial strength and feeding mechanics. *Acta Palaeontol. Pol.* **51**, 435–454.
- Summers, A.P. (2000). Stiffening the stingray skeleton – an investigation of durophagy in myliobatid stingrays (Chondrichthyes, Batoidea, Myliobatidae). *J. Morphol.* **243**, 113–126.
- Summers, A.P. & Long, J.H., Jr (2006). Skin and bones, sinew and gristle: the mechanical behavior of fish skeletal tissues. In *Fish biomechanics*: Vol. 141, 141–178. Shadwick, R.E. & Lauder, G.V. (Eds). London: Elsevier Academic Press.
- Thomason, J.J. (1995). To what extent can the mechanical environment of a bone be inferred from its internal architecture. In *Functional morphology in vertebrate paleontology*: Vol. 249, 249–263. Thomason, J.J. (Ed.). Cambridge: Cambridge University Press.
- Tricas, T.C. (1985). Feeding ethology of the white shark, *Carcharodon carcharias*. *Memoirs South. Calif. Acad. Sci.* **9**, 81–91.
- Tricas, T.C. & McCosker, J.E. (1984). Predatory behavior of the white shark (*Carcharodon carcharias*), with notes on its biology. *Proc. Calif. Acad. Sci.* **43**, 221–238.
- Turner, S. (2004). Early vertebrates: analysis from microfossil evidence. In *Recent advances in the origin and early radiation of vertebrates*: Vol. 65, 67–94. Arratia, G., Wilson, M.V.H. & Cloutier, R. (Eds). Munich: Verlag Publishing.
- Wroe, S. (2007). Cranial mechanics compared in extinct marsupial and extant African lions using a finite-element approach. *J. Zool.* **274**, 332–339.
- Wroe, S., Clausen, P., McHenry, C.R., Moreno, K. & Cunningham, E. (2007a). Computer simulation of feeding behaviour in the thylacine and dingo as a novel test for convergence and niche overlap. *Proc. Roy. Soc. Lond. Ser. B* **274**, 2819–2828.
- Wroe, S., McHenry, C. & Thomason, J. (2005). Bite club: comparative bite force in big biting mammals and the prediction of predatory behaviour in fossil taxa. *Proc. Roy. Soc. Lond. Ser. B* **272**, 619–625.
- Wroe, S., Moreno, K., Clausen, P., McHenry, C. & Curnoe, D. (2007b). High resolution three-dimensional computer simulation of hominid cranial mechanics. *Anat. Rec. Part A* **290**, 1248–1255.